AIP Journal of Applied Physics

Effects of size and concentration on diffusion-induced stress in lithium-ion batteries

Zengsheng Ma, Xiang Gao, Yan Wang, and Chunsheng Lu

Citation: Journal of Applied Physics **120**, 025302 (2016); doi: 10.1063/1.4958302
View online: http://dx.doi.org/10.1063/1.4958302
View Table of Contents: http://scitation.aip.org/content/aip/journal/jap/120/2?ver=pdfcov
Published by the AIP Publishing

Effects of size and concentration on diffusion-induced stress in lithium-ion batteries

Zengsheng Ma,[1,a)] Xiang Gao,[1] Yan Wang,[2,3] and Chunsheng Lu[3,b)]
[1]*National–Provincial Laboratory of Special Function Thin Film Materials, and School of Materials Science and Engineering, Xiangtan University, Hunan 411105, China*
[2]*School of Information and Electronic Engineering, Hunan University of Science and Technology, Hunan 411201, China*
[3]*Department of Mechanical Engineering, Curtin University, Perth, Western Australia 6845, Australia*

(Received 5 May 2016; accepted 28 June 2016; published online 8 July 2016)

Capacity fade of lithium-ion batteries induced by chemo-mechanical degradation during charge-discharge cycles is the bottleneck in design of high-performance batteries, especially high-capacity electrode materials. Stress generated due to diffusion-mechanical coupling in lithium-ion intercalation and deintercalation is accompanied by swelling, shrinking, and even micro-cracking. In this paper, we propose a theoretical model for a cylindrical nanowire electrode by combining the bond-order-length-strength and diffusion theories. It is shown that size and concentration have a significant influence on the stress fields in radial, hoop, and axial directions. This can explain why a smaller electrode with a huge volume change survives in the lithiation/delithiation process. *Published by AIP Publishing.* [http://dx.doi.org/10.1063/1.4958302]

I. INTRODUCTION

Lithium-ion batteries (LIBs) have been widely used as power devices for portable electronics.[1] Among the types of anode materials for LIBs, silicon (Si) is one of the most promising materials because of its high theoretical charging capacity ($\sim$4200 mA h g^{-1}).[2] As is known, one Si atom can host up to 4.4 Li-ions, however, such a large amount of Li absorption may result in a volume swelling of $\sim$400%, and pulverize electrodes.[3–5] Due to the diffusion-induced stress (DIS) in LIBs, there are different kinds of degradation during intercalation and deintercalation of Li-ions, such as the increase of impedance, loss of capacity, and shortage of cycle life, which has raised more concerns about failure of electrodes.[6,7] In consideration of the analogy between diffusion and heat flow, DIS can be modeled as thermal stress.[8] For example, Gao and Hong[2] developed a finite element model to calculate the DIS during lithiation. Brassart and Suo[9] suggested a chemo-mechanical yield condition, including both the DIS and driving force for reaction. Cui *et al.*[10] reported a new stress-dependent chemical potential for solid state diffusion under multiple driving forces. Recently, taking into account the Li-ion concentration distribution along the direction of radius, we calculated the DIS field based on a perfectly elastic-plastic model.[11,12]

It is indicated that the lithiation-induced deformation of electrodes can be accommodated by plastic flow when stress exceeds yield strength.[3,13,14] This makes it possible to maintain a good capacity over many cycles for electrodes with small sizes such as thin films,[15] nanowires,[16] and porous structures.[17–19] With miniaturization down to a nanometer scale, the physical properties of these materials become tunable with their shapes and feature sizes.[20–25] Cheng and Verbrugge[26] studied surface mechanisms in spherical nanoparticles and mentioned that surface stress can relieve DIS. Liu *et al.*[27] showed experimentally that, due to an insufficient amount of strain energy, there was a strong particle-size-dependent fracture behavior of Si nanoparticles during the first lithiation. Using a combination of diffusion kinetics and fracture mechanics, Zhao *et al.*[28] outlined a theory to study how material properties, particle size, and discharge rate affect fracture of electrodes in LIBs. By analyzing the stress-associated with lithiation/delithiation, Ryu *et al.*[29] successfully predicted the fracture critical size of nanowire electrodes.

Various models have been developed to mitigate adverse mechanical effects during electrochemical lithiation. As an extremely complex electrochemical reaction process, however, one of the fundamental questions on electrode charging or discharging remains unclear, that is, how to accurately describe such a multi-scale coupled problem that comprises elements of electrochemical reaction and solid mechanics at a nano or atomic scale. According to the bond-order-length-strength (BOLS) theory, if one bond breaks, the remaining ones with the lower coordinated atoms become shorter and stronger, implying that there is a strong size effect in a smaller scale.[30–32]

In this paper, the main aim is to build up a theoretical model to study the combined effects of size and concentration on the DIS in a cylindrical electrode. Further, DIS is predicted when the cylindrical electrode is at the nanoscale. Finally, possible implications of the results are discussed for prolonging the lifetime of cylindrical electrodes in LIBs.

II. THEORETICAL MODEL

As schematically illustrated in Figure 1, a cylindrical nano-electrode with radius R can be considered as a homogeneous isotropic linear elastic solid with small deformation,

[a)]Electronic mail: zsma@xtu.edu.cn
[b)]Electronic mail: c.lu@curtin.edu.au

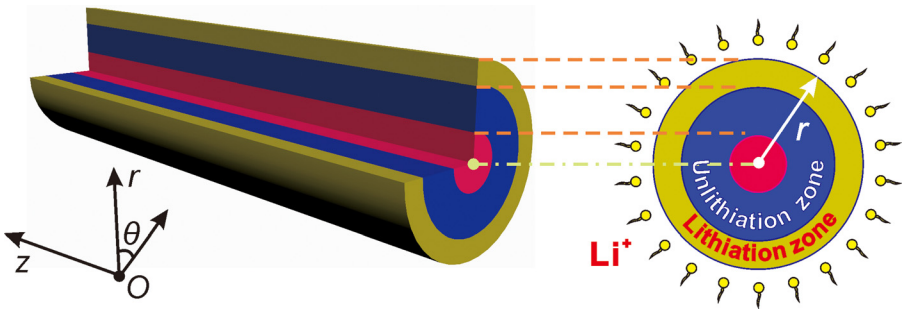

FIG. 1. Schematic illustration of Li-ion diffusion into a cylindrical electrode that causes a volume deformation.

but its mechanical properties are dependent on the solute concentration. Due to symmetry of the cylindrical electrode, there are three stress components such as the radial stress (σ_r), hoop stress (σ_θ), and axial stress (σ_z).

A. Diffusion equation

It is assumed that the Li-ion diffusion coefficient D is a constant. According to Fick's law, the diffusion of Li-ions in a cylindrical coordinate system (see Figure 1) can be written as[33]

$$\frac{\partial c(r,t)}{\partial t} = D\nabla^2 c(r,t), \tag{1}$$

where $c(r,t)$ is the Li-ion concentration at time t. During charging, Li-ions transport from an outer surface towards the current collector, and thus the boundary conditions are

$$\begin{cases} -D\dfrac{\partial c(r,t)}{\partial r}\Big|_{r=R} = -\dfrac{i}{F} \\ \dfrac{\partial c(r,t)}{\partial r}\Big|_{r=0} = 0, \end{cases} \tag{2}$$

where i is the surface current density and F is Faraday's constant. According to Cheng and Verbrugge,[22] the Li-ion flux on the electrode surface can be expressed as

$$\frac{i}{F} = (\omega_a + \omega_c)\left[c_f - \frac{\omega_c}{\omega_a + \omega_c}\right], \tag{3}$$

$$c_f = c_R/c', \tag{4}$$

where ω_a and ω_c are interface rate constants, c_f is the concentration (fractional occupancy) of a filled host site, and c' denotes the total site concentration available for guest insertion in an electrode. For the simplification of analysis, three dimensionless parameters are defined as

$$\begin{cases} \bar{t} = \dfrac{Dt}{R^2} \\ \bar{r} = \dfrac{r}{R} \\ \overline{Bi} = \dfrac{(\omega_a + \omega_c)R}{Dc'}, \end{cases} \tag{5}$$

where, similar to one in a heat-transfer system, $\overline{Bi}$ is the so-called electrochemical Biot number. Here, it is worth noting that the Biot number is a dimensionless quantity and a measure of the relative importance of heat flow within a body in comparison to heat flow on the surface. The electrochemical Biot number $\overline{Bi}$ can be viewed as the ratio of the solute (Li) diffusion resistance to that of the overall charge-transfer process.[34,35] A larger Biot number represents a system whose kinetics is limited by diffusion, whereas a smaller Biot number refers to a system governed by the charge-transfer process. Thus, the dimensionless concentration $\bar{c}$ can be represented as

$$\bar{c}\left(\bar{r},\bar{t},\overline{Bi}\right) = \frac{c(r,t)}{c_R}. \tag{6}$$

The Li-ion concentration (c_R) on the surface of an electrode is

$$c_R = c'\frac{\omega_c}{\omega_a + \omega_c}. \tag{7}$$

Considering the initial condition, $c(r,0) = 0$, and substituting Eqs. (2)–(7) into Eq. (1), the solution can be obtained as[29]

$$\bar{c}\left(\bar{r},\bar{t},\overline{Bi}\right) = 1 - 2\sum_{\kappa=1}^{\infty}\frac{\overline{Bi}}{\left(\zeta_\kappa^2 + \overline{Bi}_\kappa^2\right)}\frac{J_0(\zeta_\kappa \bar{r})}{J_0(\zeta_\kappa)}\exp\left(-\zeta_\kappa^2 \bar{t}\right), \tag{8}$$

where ζ_κ is the κth zero of the first-order Bessel function (J) of the first kind, that is

$$\overline{Bi}\,J_0(\zeta_\kappa) - \zeta_\kappa J_1(\zeta_\kappa) = 0. \tag{9}$$

B. Stress with transformation strain

In a cylindrical coordinate system, the strain components are defined as

$$\varepsilon_r = \frac{du}{dr}, \qquad \varepsilon_\theta = \frac{du}{r}, \tag{10}$$

where u is the radial displacement, and ε_r and ε_θ are strain components along the radial and hoop directions, respectively. The constitutive equations associated with solute concentration can be described as[29]

$$\begin{cases} \varepsilon_r = \dfrac{1}{E}[\sigma_r - \nu(\sigma_\theta + \sigma_z)] + \dfrac{1}{3}\Omega c(r,t) \\ \varepsilon_\theta = \dfrac{1}{E}[\sigma_\theta - \nu(\sigma_z + \sigma_r)] + \dfrac{1}{3}\Omega c(r,t) \\ \varepsilon_z = \dfrac{1}{E}[\sigma_z - \nu(\sigma_r + \sigma_\theta)] + \dfrac{1}{3}\Omega c(r,t), \end{cases} \tag{11}$$

where ε_z is strain along the axial direction, E is Young' modulus, ν is Poisson's ratio, and Ω is the partial molar volume. σ_r, σ_θ, and σ_z are stress components along the radial, hoop, and axial directions, respectively. The equilibrium equation in such an axisymmetric case can be represented as

$$\frac{\partial \sigma_r}{\partial r} + \frac{\sigma_r - \sigma_\theta}{r} = 0. \tag{12}$$

Generally, the cylindrical electrode is treated as a long wire and according to the plane strain assumption,[33] we have

$$\varepsilon_z = 0. \tag{13}$$

Based on Eqs. (10)–(13), the radial displacement u can be determined by

$$\frac{\partial^2 u}{\partial r^2} + \frac{1}{r}\frac{\partial u}{\partial r} - \frac{u}{r^2} = \frac{(1+\nu)\Omega}{3(1-\nu)}\frac{\partial c(r,t)}{\partial r}. \tag{14}$$

The boundary conditions are given as

$$\sigma(r,t)|_{r=R} = 0, \quad u(r,t)|_{r=0} = 0. \tag{15}$$

By solving the elastic boundary-value problem as described in Eqs. (10)–(15), the radial, tangential, and axial stresses can be obtained as

$$\sigma_r = \frac{E\Omega}{3(1-\nu)}\left[\frac{1}{R^2}\int_0^R rc(r,t)dr - \frac{1}{r^2}\int_0^r rc(r,t)dr\right], \tag{16}$$

$$\sigma_\theta = \frac{E\Omega}{3(1-\nu)}\left[\frac{1}{R^2}\int_0^R rc(r,t)dr + \frac{1}{r^2}\int_0^r rc(r,t)dr - c(r,t)\right], \tag{17}$$

$$\sigma_z = \frac{E\Omega}{3(1-\nu)}\left[\frac{2\nu}{R^2}\int_0^R rc(r,t)dr - c(r,t)\right]. \tag{18}$$

C. Bond-order-length-strength (BOLS) theory

According to the BOLS theory, the size dependence of elastic modulus originates from the broken-bond-induced local strain and skin depth energy pinning.[36] As an extension of the atomic "coordination-radius" correlation premise of Pauling and Goldschmidt,[37,38] the BOLS theory can be expressed as

$$\begin{cases} C_i = \dfrac{d_i}{d_b} = \dfrac{2}{1+\exp[(12-z_i)/(8z_i)]} & \text{(BOLS-coefficient)} \\ E_i = C_i^{-m} E_b & \text{(Single-bond-energy)} \\ E_{Bi} = z_i E_i & \text{(Atomic-coherency)}, \end{cases} \tag{19}$$

where C_i and d are the coefficients of bond contraction and bond length, subscripts i and b denote an atom in the ith atomic layer and bulk, respectively, and as illustrated in Figure 2, i is counted up to three from the outermost inward.[39] Here, it is worth noting that C_i is anisotropic and depends on the effective coordination number. The index m is an indicator of bond for a given material, which may embed the electronegativity difference and iconicity (or the extent of chemical bond formation) of a compound. For Si, the optimized m value is 4.88.[40] E_{Bi} indicates the atomic cohesive energy of an atom in the ith layer, which is defined as the product of the atomic coordination number and bond energy. z_i is the effective coordination number of the ith atom and varies with the size and curvature of a nanostructure, which can be empirically determined by

$$\begin{cases} z_1 = \begin{cases} 4(1-0.75/K) & \text{(Curved-surface)} \\ 4 & \text{(Flat-surface)} \end{cases} \\ z_2 = z_1 + 2 \\ z_3 = 12, \end{cases} \tag{20}$$

where $K = R/d_0$ (d_0 is the average bond length) is the number of atoms lined along the radius of a nanosphere (the thickness of a thin film or a nanowire), as shown in Figure 2. Substituting Eq. (20) into (19), we can get a general form, that is

$$\frac{\Delta E}{E_B} = \frac{E - E_B}{E_B} = \frac{\tau d_0}{R}\left[\sum_{i\le 3} C_i\left(C_i^{-(m+3)} - 1\right)\right], \tag{21}$$

where ΔE is the change of Young's modulus (E) with respect to the standard bulk value (E_B), and $\tau = 1$, 2, and 3 are corresponding to a thin film, a cylindrical rod, and a spherical particle, respectively.[21,41] Here, let us introduce a size effect factor χ_s, and then Eq. (21) becomes

$$E = E_B(1+\chi_s). \tag{22}$$

The dimensionless parameter χ_s can be written as

$$\chi_s = \frac{\tau d_0}{R}\left[\sum_{i\le 3} C_i\left(C_i^{-(m+3)} - 1\right)\right]. \tag{23}$$

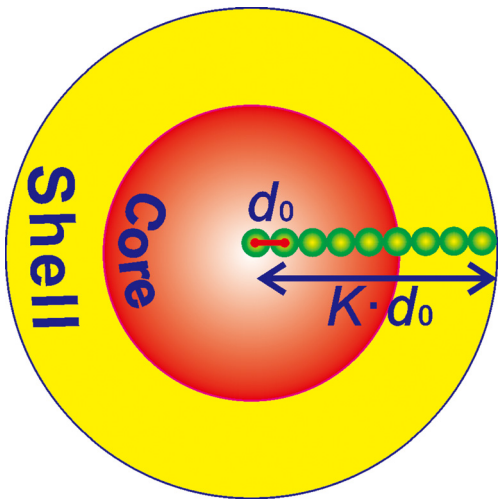

FIG. 2. Illustration of the core-shell structure and dimensionless size of K.

Because the relationship of Young's modulus and concentration is described by linear functions,[42] the other dimensionless factor χ_c is defined to represent the concentration dependency of Young's modulus, that is

$$E_B = E_0(1+\chi_c), \tag{24}$$

where E_0 is Young's modulus without the influence of concentration. According to Yang,[43]

$$\chi_c = \alpha c(r,t)/E_0, \tag{25}$$

where α is the change of Young's modulus per unit concentration of solute atoms. In terms of Eqs. (22) and (24), we have

$$E = E_0(1+\chi_c)(1+\chi_s). \tag{26}$$

Substituting Eq. (26) into Eqs. (16)–(18), the radial, hoop, and axial dimensionless stresses can be rearranged as

$$\begin{aligned}\hat{\sigma}_r &= \frac{\sigma_r}{E_0\Omega c_R/3(1-\nu)} \\ &= -2(1+\chi_c)(1+\chi_s) \\ &\quad\times\sum_{\kappa=1}^{\infty}\frac{\overline{Bi}}{\bar{r}\left(\zeta_\kappa^2+\overline{Bi}_\kappa^2\right)\zeta_\kappa}\frac{\bar{r}J_1(\zeta_\kappa)-J_1(\zeta_\kappa\bar{r})}{J_0(\zeta_\kappa)}\exp\left(-\zeta_\kappa^2\bar{t}\right),\end{aligned} \tag{27}$$

$$\begin{aligned}\hat{\sigma}_\theta &= \frac{\sigma_\theta}{E_0\Omega c_R/3(1-\nu)} \\ &= -2(1+\chi_c)(1+\chi_s) \\ &\quad\times\sum_{\kappa=1}^{\infty}\frac{\overline{Bi}}{\bar{r}\left(\zeta_\kappa^2+\overline{Bi}_\kappa^2\right)\zeta_\kappa}\frac{\bar{r}J_1(\zeta_\kappa)+J_1(\zeta_\kappa\bar{r})-\zeta_\kappa\bar{r}J_0(\zeta_\kappa\bar{r})}{J_0(\zeta_\kappa)} \\ &\quad\times\exp\left(-\zeta_\kappa^2\bar{t}\right),\end{aligned} \tag{28}$$

$$\begin{aligned}\hat{\sigma}_z &= \frac{\sigma_z}{E_0\Omega c_R/3(1-\nu)} \\ &= -(1+\chi_c)(1+\chi_s) \\ &\quad\times\left[(1-\nu)+2\sum_{\kappa=1}^{\infty}\frac{\overline{Bi}}{\left(\zeta_\kappa^2+\overline{Bi}_\kappa^2\right)\zeta_\kappa}\right. \\ &\quad\left.\times\frac{2\nu J_1(\zeta_\kappa)-\zeta_\kappa J_0(\zeta_\kappa\bar{r})}{J_0(\zeta_\kappa)}\exp\left(-\zeta_\kappa^2\bar{t}\right)\right].\end{aligned} \tag{29}$$

III. RESULTS AND DISCUSSION

As shown in Figure 3, the Li-ion concentration rises continuously with the increase of time and radial location. For a smaller Biot number of 0.01 in Figure 3(a), concentration is rather low (~0) because the electrode operates under a large interfacial resistance and needs a long time to be

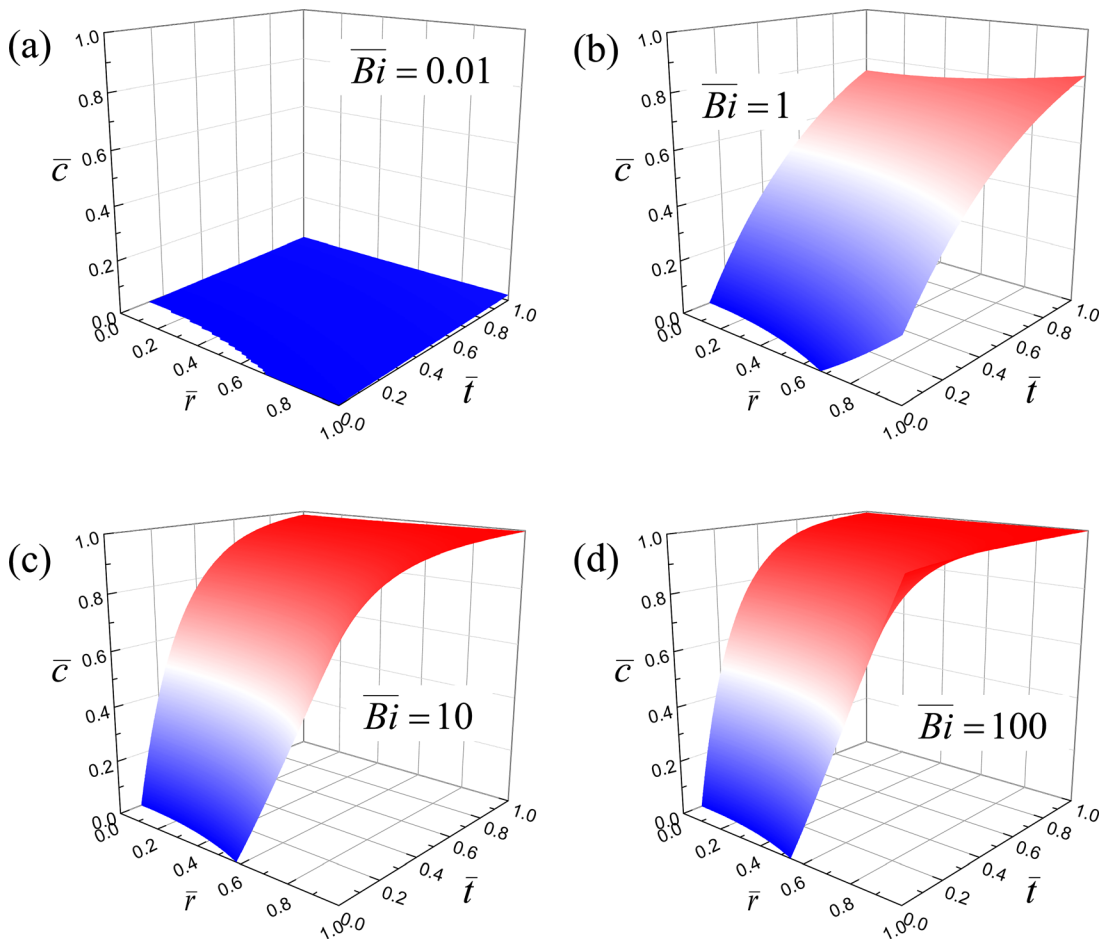

FIG. 3. The dimensionless Li-ion concentration at different radial locations and times with the Biot number of (a) $\overline{Bi}=0.01$, (b) $\overline{Bi}=1$, (c) $\overline{Bi}=10$, and (d) $\overline{Bi}=100$.

fully charged. When the Biot number increases to 1 (see Figure 3(b)), the electrode is charged under a small interfacial resistance and charging is completed in a short time. Even at the initial time $\bar{t} = 0$, Li-ions have diffused into the electrode. As shown in Figures 3(c) and 3(d), concentration quickly increases to 1. Therefore, the Biot number can be used to describe the whole progress of Li-ion diffusion, which plays a significant role in design of an insertable electrode.

In the absence of size effect ($\chi_s = 0$), the distributions of radial, hoop, and axial stresses versus the radial location at different times are shown in Figures 4(a)–4(e), respectively. Taking into account no concentration (see Figure 4(a)), the radial stress is always tensile and becomes zero on the electrode surface. The stress continuously increases to the maximum value at its center, which is in agreement with previous results.[26,44] Obviously, the Biot number largely affects the distribution of radial stress during charging. As shown in Figure 4(c), the maximum tensile hoop stress appears at the center of an electrode while the maximum compressive stress is on the surface. When solute reaches approximately half of the electrode radius, compressive tangential stress turns into tension. Furthermore, with the increase of time, hoop stress increases, implying that the cylinder electrode is prone to fracture in a higher charging state. As shown in Figure 4(e), axial stress is always compressive no matter

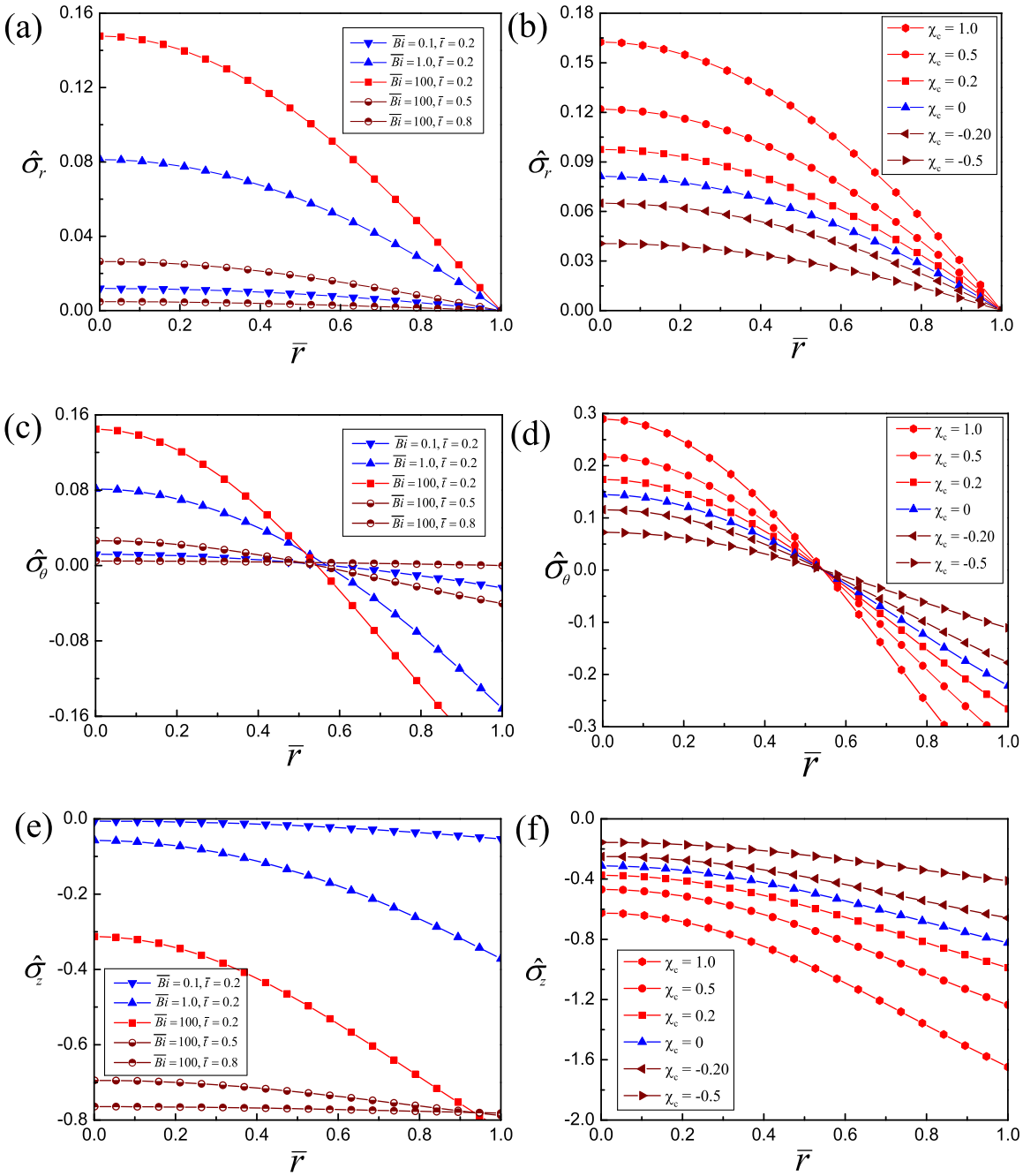

FIG. 4. Without size effect, the dimensionless stress of (a) σ_r, (c) σ_θ, and (e) σ_z versus the dimensionless radial $\bar{r}$; and the influence of concentration on dimensionless stress of (b) σ_r, (d) σ_θ, and (f) σ_z under $\overline{Bi} = 100$ and $\bar{t} = 0.2$.

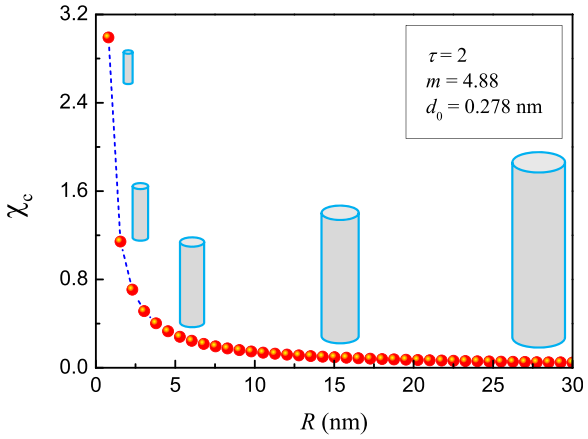

FIG. 5. Without concentration effect, the dimensionless parameter χ_s versus the cylindrical radius R.

what the Biot number and time are. As charging goes on, the axial stress tends to be a steady compressive state.

To investigate the influence of concentration, we choose the χ_c value from −0.5 to 1.0, corresponding to material softening (negative) and hardening (positive), respectively. As shown in Figures 4(b), 4(d), and 4(f), it is obvious that concentration plays an important role in determining the stress distribution.

Figure 5 shows the theoretical prediction on the size dependence of χ_c in Si nanowires by using parameters listed in Table I. It is seen that χ_c increases from zero to infinite with the decrease of nanowire radius, especially at a very small size of $R < 10$ nm. The theoretical prediction of Si nanowires is consistent with experimental results measured from zinc oxide and silver nanowires,[45,46] and obtained by our previous study.[47] Without concentration effect, the distribution of stress is calculated as a function of position R ranging from 3 nm to infinite, as shown in Figure 6. It is observed that, with the decrease of R, all these stresses increase. When R increases to infinite, however, stress approaches to that of no size effect. That is, in the case of R being beyond 50 nm, the size effect can be ignored, which is attributed to the reduction of surface effect. Therefore, the gradual decrease of nanowire size results in an enormous increase of Young's modulus. Generally speaking, the smaller the electrode, the lower its DIS is.[20,26,33,48] The current outcome seems to be in contradiction with this viewpoint. Essentially, when the radius of an electrode is less than 50 nm, the size effect determines the stress increase based on the BOLS theory. However, when its radius is beyond 50 nm, stress degeneration happens with the decrease of radius, which can be attributed to the plastic flow and two-phase lithiation mechanism.

TABLE I. Material properties and operating parameters.

Parameter	Symbol	Value
Diffusion coefficient	D (m^2 s^{-1})	12×10^{-18}
Maximum stoichiometric Li concentration	c_R (#/nm^3)	53.398
Partial molar volume of solute	Ω (nm^3/#)	0.014
Lattice constant of Si–Li	d_0 (nm)	0.278
Poisson's ratio	ν	0.228
Indicator of the Si bond	m	4.88
Shape factor of a cylinder	τ	2

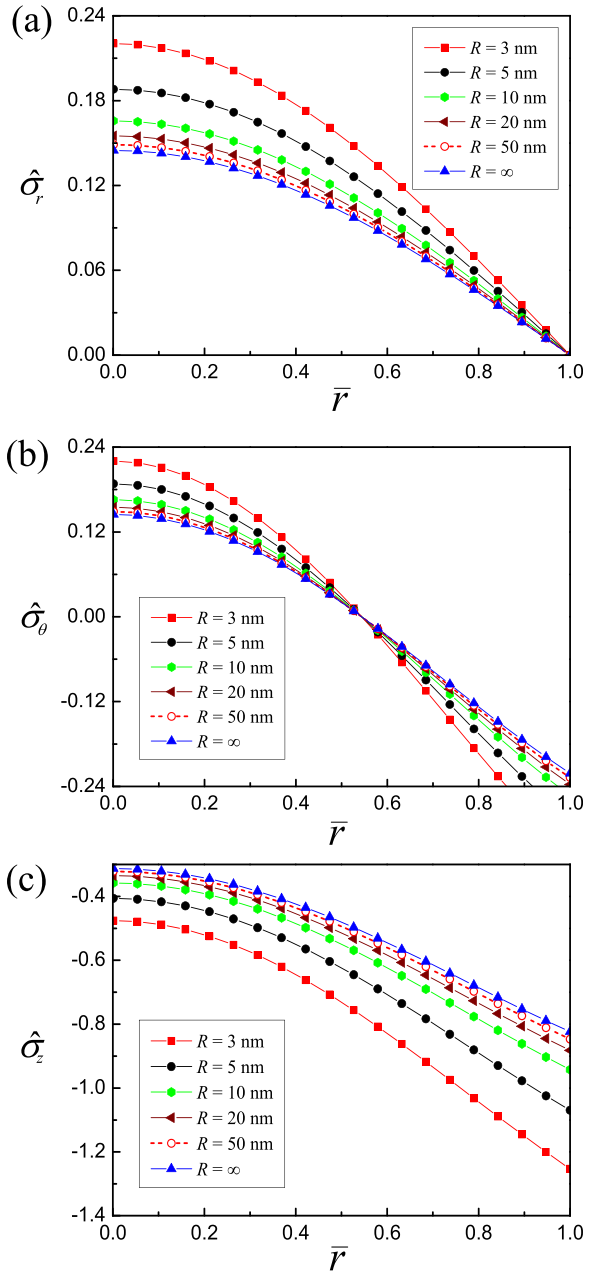

FIG. 6. With no concentration effect, the dimensionless stress of (a) σ_r, (b) σ_θ, and (c) σ_z versus the dimensionless radial $\bar{r}$ under $\overline{Bi} = 100$ and $\bar{t} = 0.2$ with different cylindrical radii of R.

IV. CONCLUSIONS

In summary, by combining the BOLS and diffusion theories, we have developed a theoretical model to study stress fields in a cylindrical nanowire electrode. It is shown that size and concentration have a significant influence on the stress fields in radial, hoop, and axial directions. The tensile radial stress decreases from the maximum value at the center to zero on surface, the hoop stress becomes compression in the middle of radius, and the compressive axial stress continuously increases. This could improve the stability and

reliability of LIBs. Thus, a good understanding on the stress field evolution and effects of size and concentration has general implications for building reliable batteries through design optimization of electrode materials.

ACKNOWLEDGMENTS

This work was supported by the National Natural Science Foundation of China (Grant Nos. 11372267, 11402086, and 11472141).

[1]R. Van Noorden, Nature **507**, 26 (2014).
[2]F. Gao and W. Hong, J. Mech. Phys. Solids **94**, 18 (2016).
[3]K. Zhao, W. L. Wang, J. Gregoire, M. Pharr, Z. Suo, J. J. Vlassak, and E. Kaxiras, Nano Lett. **11**, 2962 (2011).
[4]Y. Song, B. Lu, X. Ji, and J. Zhang, J. Electrochem. Soc. **159**, A2060 (2012).
[5]H. Yang, W. Liang, X. Guo, C. M. Wang, and S. Zhang, Extreme Mech. Lett. **2**, 1 (2015).
[6]J. Vetter, P. Novák, M. Wagner, C. Veit, K. C. Möller, J. Besenhard, M. Winter, M. Wohlfahrt-Mehrens, C. Vogler, and A. Hammouche, J. Power Sources **147**, 269 (2005).
[7]X. Gao, Z. Ma, W. Jiang, P. Zhang, Y. Wang, Y. Pan, and C. Lu, J. Power Sources **311**, 21 (2016).
[8]S. Prussin, J. Appl. Phys. **32**, 1876 (1961).
[9]L. Brassart and Z. Suo, J. Mech. Phys. Solids **61**, 61 (2013).
[10]Z. Cui, F. Gao, and J. Qu, J. Mech. Phys. Solids **60**, 1280 (2012).
[11]Z. S. Ma, Z. C. Xie, Y. Wang, P. P. Zhang, Y. Pan, Y. C. Zhou, and C. Lu, J. Power Sources **290**, 114 (2015).
[12]Z. Xie, Z. Ma, Y. Wang, Y. Zhou, and C. Lu, RSC Adv. **6**, 22383 (2016).
[13]V. A. Sethuraman, M. J. Chon, M. Shimshak, V. Srinivasan, and P. R. Guduru, J. Power Sources **195**, 5062 (2010).
[14]P. Zhang, Z. Ma, W. Jiang, Y. Wang, Y. Pan, and C. Lu, AIP Adv. **6**, 015107 (2016).
[15]P. R. Abel, Y. M. Lin, H. Celio, A. Heller, and C. B. Mullins, ACS Nano **6**, 2506 (2012).
[16]K. Chen and D. Xue, J. Phys. Chem. C **117**, 22576 (2013).
[17]P. G. Bruce, B. Scrosati, and J. M. Tarascon, Angew. Chem. Int. Ed. **47**, 2930 (2008).
[18]K. Chen, F. Liu, S. Song, and D. Xue, CrystEngComm **16**, 7771 (2014).
[19]K. Chen and D. Xue, Sci. Sin. Tech. **45**, 36 (2015).
[20]R. Dingreville, J. Qu, and C. Mohammed, J. Mech. Phys. Solids **53**, 1827 (2005).
[21]J. Li, S. Ma, X. Liu, Z. Zhou, and C. Q. Sun, Chem. Rev. **112**, 2833 (2012).
[22]Y. T. Cheng and M. W. Verbrugge, J. Electrochem. Soc. **157**, A508 (2010).
[23]K. Chen and D. Xue, Sci. China Technol. Sci. **58**, 1768 (2015).
[24]F. Liu and D. Xue, Sci. China Technol. Sci. **58**, 1841 (2015).
[25]K. Chen, S. Song, F. Liu, and D. Xue, Chem. Soc. Rev. **44**, 6230 (2015).
[26]Y. T. Cheng and M. W. Verbrugge, J. Appl. Phys. **104**, 083521 (2008).
[27]X. H. Liu, L. Zhong, S. Huang, S. X. Mao, T. Zhu, and J. Y. Huang, ACS Nano **6**, 1522 (2012).
[28]K. Zhao, M. Pharr, J. J. Vlassak, and Z. Suo, J. Appl. Phys. **108**, 073517 (2010).
[29]I. Ryu, J. W. Choi, Y. Cui, and W. D. Nix, J. Mech. Phys. Solids **59**, 1717 (2011).
[30]C. Q. Sun, Prog. Solid State Chem. **35**, 1 (2007).
[31]C. Q. Sun, Phys. Rev. B **69**, 045105 (2004).
[32]Z. Ma, S. Long, Y. Pan, and Y. Zhou, J. Appl. Phys. **103**, 043512 (2008).
[33]R. Deshpande, Y. T. Cheng, and M. W. Verbrugge, J. Power Sources **195**, 5081 (2010).
[34]J. Li, X. Xiao, Y. T. Cheng, and M. W. Verbrugge, J. Phys. Chem. Lett. **4**, 3387 (2013).
[35]T. Hatchard, D. MacNeil, A. Basu, and J. Dahn, J. Electrochem. Soc. **148**, A755 (2001).
[36]C. Q. Sun, Prog. Mater. Sci. **54**, 179 (2009).
[37]L. Pauling, J. Am. Chem. Soc. **69**, 542 (1947).
[38]V. Goldschmidt, Ber. Derch. Chem. Ges. **60**, 1263 (1927).
[39]W. Huang, R. Sun, J. Tao, L. Menard, R. Nuzzo, and J. Zuo, Nat. Mater. **7**, 308 (2008).
[40]L. Pan and C. Q. Sun, J. Appl. Phys. **95**, 3819 (2004).
[41]Z. Ma, T. Li, Y. Huang, J. Liu, Y. Zhou, and D. Xue, RSC Adv. **3**, 7398 (2013).
[42]Y. Li, K. Zhang, and B. Zheng, J. Electrochem. Soc. **162**, A223 (2015).
[43]F. Yang, Sci. China Phys. Mech. **55**, 955 (2012).
[44]X. Li, Q. Fang, J. Li, H. Wu, Y. Liu, and P. Wen, Solid State Ionics **281**, 21 (2015).
[45]C. Chen, Y. Shi, Y. Zhang, J. Zhu, and Y. Yan, Phys. Rev. Lett. **96**, 075505 (2006).
[46]G. Y. Jing, H. L. Duan, X. M. Sun, Z. S. Zhang, J. Xu, Y. D. Li, J. X. Wang, and D. P. Yu, Phys. Rev. B **73**, 235409 (2006).
[47]Z. Ma, Z. Zhou, Y. Huang, Y. Zhou, and C. Q. Sun, Sci. China Phys. Mech. **55**, 963 (2012).
[48]C. Wang, Z. Ma, Y. Wang, and C. Lu, J. Electrochem. Soc. **163**, A1157 (2016).